Journal of Biosciences and Medicines, 2022, 10, 134-150
https://www.scirp.org/journal/jbm
ISSN Online: 2327-509X
ISSN Print: 2327-5081

Preparation of Pickering Emulsion for Antibacterial, Anti-Inflammatory and Wound Healing

Jinze Pei, Ning Wei, Congcong Cui, Guangshan Xuan*

College of Chemical Engineering, Qingdao University of Science & Technology, Qingdao, China
Email: *xuan@qust.edu.cn

How to cite this paper: Pei, J.Z., Wei, N., Cui, C.C. and Xuan, G.S. (2022) Preparation of Pickering Emulsion for Antibacterial, Anti-Inflammatory and Wound Healing. *Journal of Biosciences and Medicines*, **10**, 134-150.
https://doi.org/10.4236/jbm.2022.1012012

Received: October 26, 2022
Accepted: December 20, 2022
Published: December 23, 2022

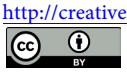

Abstract

In recent years, natural biodegradable nanoparticles as stabilizers of Pickering emulsions have attracted extensive attention. In this work, a Pickering emulsion composed of chitosan/Arabic gum nanoparticles (CS/GA NPs), tea tree oil and vitamin E was formulated. Then the antibacterial, anti-inflammatory and wound healing abilities of the emulsion were evaluated. Pickering emulsion encapsulated the tea tree oil strengthened antibacterial activity towards *Staphylococcus aureus*, *Escherichia coli*, *Pseudomonas aeruginosa* and *Candida albicans*. Besides, this multi-phase system offered a platform to load with vitamin E, which provides anti-inflammatory effects while antibacterial. Meanwhile, Pickering emulsion avoided contact between bacteria and skin when used in wound treatment.

Keywords

Pickering Emulsion, CS/GA Nanoparticles, Tea Tree Oil, Vitamin E, Antibacterial, Anti-Inflammatory, Wound Healing

1. Introduction

Wound healing is a complex process that generally involves four sequential processes such as hemostasis, anti-inflammation, new blood vessel formation and new tissue maturation. Rapid restoration of the skin to its integrity can limit dehydration and prevent the development of infection [1] [2] [3]. This requires the synergistic action of antibacterial [4] [5], anti-inflammatory [6] and substances that promote fibroblast proliferation [7].

Pickering emulsions are stabilized by solid particles [8]. The multi-component system consisting of particles, aqueous and oil phases allows Pickering emul-

sions to be loaded with both hydrophilic and hydrophobic drugs to improve their solubility and effectiveness [9]. In addition, solid particle stabilized Pickering emulsions have higher biosafety and biocompatibility than conventional surfactants stabilized classical emulsions [10]. Therefore, these properties promote the application of Pickering emulsions in the field of biomedical materials. When Pickering emulsions are used as wound dressings in direct contact with defective skin, it avoids the hemolytic, irritating, and toxic properties caused by traditional surfactants. In addition, the special structure of the solid particle shell allows Pickering emulsions to have a slow release.

Natural tea tree oil has high antibacterial, analgesic and scar inhibiting properties [9], and when used as an antimicrobial agent, natural oils do not cause any resistance and are safer than traditional antibiotics [11] [12] [13]. Chitosan has excellent adhesive properties and has various positive effects on wound healing, such as hemostasis, accelerated tissue regeneration, and promotion of fibroblast proliferation [14] [15]. Gum Arabic has good film-forming properties, protects the skin from lipid peroxidation caused by continuous exposure to UV light, and has the effect of preventing premature skin aging [16]. Vitamin E has antioxidant and anti-inflammatory effects [17] [18].

In this study, we intend to use the antibacterial effect of tea tree oil, the antioxidant effect of VE and the stabilizing effect of chitosan/Acacia gum nanoparticles to develop Pickering emulsion with antibacterial, anti-inflammatory and wound healing promoting properties.

2. Materials and Methods

2.1. Materials

Chitosan powder was purchased from Haizhiyuan Co., China; Gum Arabic, Tea tree oil, and VE were procured from Shanghai McLean Reagent Co., Ltd; Acetic acid was purchased from Tianjin Bodi Chemical Co., Ltd. The other reagents used were analytically pure grade.

Kunming mice, 20 g of weight, were obtained from Qingdao experimental animal and animal experiment center (Qingdao, China). This study was performed in strict accordance with the Regulations for the Care and Use of Laboratory Animals and Guideline for Ethical Review of Animal (China, GB/T 35892-2018). All animal experiments were reviewed and approved by the Animal Ethics Committee of the Institute of Process Engineering (approval ID: SCXK(LU)2020-0007).

2.2. Methods

2.2.1. Preparation of CS/GA Nanoparticles and Pickering Emulsion

Dissolve the required amount of chitosan in 1% acetic acid, then dissolve the corresponding weight of Arabic gum in the same volume of deionized water. Drop the Arabic gum solution into the chitosan solution with constant magnetic stirring to prepare CS/GA nanoparticle (CS/GA NPs) dispersion with a concen-

tration of 1.5%, ratio of 1:4, 1:2, 4:1 and 2:1. Same way to prepare CS/GA nanoparticle dispersion with ratio of 1:1 and concentration of 0.5%, 1.0%, 2.0% and 3.0% respectively.

Tea tree oil was selected as the oil phase because of its excellent properties for wound healing, including antibacterial activity, anti-inflammatory properties and scar prevention properties [19]. Pickering emulsions (PE) were prepared by homogenization. The process was carried out at a pressure of 400 MPa for 5 min. Then different proportions and concentrations of nanoparticle dispersion and different volumes of tea tree oil were used to prepare Pickering emulsion. Same way to prepare the classical emulsion (CE), but no CS/GA nanoparticles.

VE was selected as its wonderful anti-inflammatory property [18]. Dissolved VE into tea tree oil. Prepared the VE-Pickering emulsion (VE-PE) with the concentration of 1.5% nanoparticle dispersion and a mass ratio of 1:1 CS/GA, which is the stable ratio to this emulsion in previous pre-experiments. Same way to prepare the VE-classical emulsion (VE-CE).

2.2.2. Characterization of CS/GA Nanoparticles and Pickering Emulsion

The infrared spectra of CS, GA and CS/GA were measured by potassium bromide (KBr) tablet pressing method and measured by FT-IR 8400 Fourier infrared spectrometer. The scanning was carried out in the range of 400 - 4000 cm^{-1} with a resolution of 2 cm^{-1}.

The average size of the formed nanoparticles was measured using Zetasizer Nano ZS zen3600. The sample is diluted 100 times with deionized water, and the reported result is the average of three consecutive readings.

The contact angle of the formed nanoparticles was measured using a contact angle meter. The sample shall be evenly coated on the glass plate, dried at 50˚C. Add 5 μL of deionized water dropwise with a high-precision syringe, and measure the contact angle.

The morphology of nanoparticles was analyzed by HT7800 transmission electron microscope. The prepared nanoparticle dispersions were deposited on a copper grid and observed after evaporation of the liquid by mercury lamp irradiation.

The creaming index (CI) was observed and measured 7 days, 14 days, 21 days and 30 days after the preparation of the emulsion so as to evaluate the long-term stability of Pickering emulsion. Creaming index = height of water layer/total height of emulsion solution.

2.2.3. Entrapment Efficiency and Loading Content

Encapsulation efficiency (EE %) and drug loading (LC %) were determined to evaluate VE retention in core oil droplets. Briefly, 1 g of the prepared emulsion was diluted in 9 mL of methanol and ultrasound for 15 min to break the emulsion. After filtration with a 0.22 μm microporous membrane, 1 mL of the prepared emulsion was diluted 10 times with methanol and measured absorbance at 282 nm. The total amount of VE in the emulsion was calculated from the VE

standard curve.

Another 1 g of emulsion was diluted tenfold in 9 mL of distilled water, centrifuged at 4000 rpm for 10 min to separate the water layer from the oil layer, and the quantitative analysis of the drug (free VE) in the aqueous layer was performed by UV spectrophotometer. Then calculate EE % and LC % with Equations (1) and (2).

$$\mathrm{EE}(\%) = \frac{\text{total amount of VE-free}}{\text{total amount of VE}} \times 100 \tag{1}$$

$$\mathrm{LC}(\%) = \frac{\text{total amount of VE-free}}{\text{total amount of VE}} \times 100 \tag{2}$$

2.2.4. *In Vitro* Vitamin E Release Study

To access the transdermal absorption effect of the Pickering emulsion, we created mouse back skin without subcutaneous tissue and fat. The receiving solution was 100 mm pH 7.4 phosphate buffer. Put 200 μL VE-PE in the Supply cell of Franz vertical diffusion cell, and conducted the transdermal test at the condition of 32˚C and 300 rpm. Take a sample of 1 mL at 0.5, 1, 2, 4, 6, 8, 12 and 24 hours respectively, and replenish the same amount of blank receiving medium at the same temperature.

The cumulative permeability was calculated according to Equation (3).

$$Q_n = \left(C_n \times V_0 + \sum_{i=1}^{n-1} C_i \times V_i \right) \Big/ A \tag{3}$$

where Q_n referred to the cumulative permeability at the nth hour, V_0 referred to the volume of the receptor chamber, C_n and C_i referred to the sample concentration measured at the nth and ith hours, V_i referred to the volume of each sampling, and A was the diffusion area.

Drew the cumulative release time curve of VE in VE-PE and VE-CE within 24 hours, and used origin9.0 software to fit the zero order equation, first order equation, Higuchi equation and Ritger-Peppas equation to determine the release model.

2.2.5. *In Vitro* Bacteriostatic Test

The *Escherichia coli*, *Staphylococcus aureus*, *Pseudomonas aeruginosa and Candida albicans* were chosen for this antibacterial activity test. For the quantitative analysis, the bacterial suspensions previously cultured and diluted were divided into five groups and then were separately treated with 1) Tea tree oil, 2) CE, 3) Olive oil, 4) CS/GA NPs and 5) PE, as shown in Table 1. Then the five groups were incubated for 18 - 24 hours. The temperature was adjusted to the optimum temperature for each strain of bacteria. Finally, the biomass analysis was taken by measuring the size of the inhibition zone.

2.2.6. *In Vivo* Anti-Inflammatory Test

To assess the anti-inflammatory activity of the Pickering emulsion *in Vivo*, we designed an acetic acid-induced peritoneal vascular permeability test in mice. The

Table 1. Creaming index, particle size and particle size change rate of Pickering emulsion within 30 days.

Group			CI of 30 ds (%)	Diameter (nm)		Change rate (%)
CS/GA concentration	Oil ratio	CS/GA ratio		0 d	30 d	
1.5%	40%	1:4	13.514	503.9	534.2	6.01
		1:2	8.108	412.9	446.1	8.04
		1:1	0	414.1	435.4	5.14
		2:1	2.778	421.1	443.5	5.32
		4:1	5.405	514.7	557.3	8.28
0.5%	40%	1:1	65.714	568.3	840.6	47.91
1.5%			13.889	414.1	435.4	5.14
3.0%			0	1339	1390	3.81
1.5%	20%	1:1	13.889	593.6	647.7	9.11
	40%		0	414.1	435.4	5.14
	60%		0	626.0	645.3	3.08

mice were divided into five groups with five mice in each group and were separately treated with normal saline, compound dexamethasone acetate cream (2.4 g/kg), VE Pickering emulsion of high (4.8 g/kg), medium (2.4 g/kg) and low (1.2 g/kg) dose. Administered the drug for 7 days, once a day. Two hours after the last administration, heated the tail of the mice and injected 0.5% Evans blue (0.1 mL/10g) as a marker of peritoneal capillary permeability. After 10 min, inject 1.2% glacial acetic acid (0.1 mL/10g) intraperitoneally. Then collected peritoneal lavage fluid, was centrifuged at 3000 rpm for 15 min, and measured the absorbance at 610 nm with UV spectrophotometer. The peritoneal Evans blue content of each mouse was calculated according to the standard curve.

The inhibition rate of intraperitoneal exudation of mice in the administration group was calculated by taking the exudation amount of the dye in the blank group as 100%. Permeability is expressed as inhibition rate value. The inhibition rate was calculated by Equation (4), where C_0 was the exudation volume of the control group, C_1 was the exudation volume of the treatment group.

$$\text{Inhibition rate}(\%) = \frac{C_0 - C_1}{C_0} \times 100 \tag{4}$$

2.2.7. Wound Healing Test

Created full-thickness skin wounds with a diameter of 5 mm on the back of mice with sterilized scissors. After that, the mice were divided into five groups with five mice in each group and were treated with the PE, CE, CS/GA NPs, tea tree oil and normal saline, respectively. Apply the drug twice a day according to the amount of 2.4 g/kg for 10 consecutive days. Photographs of the wounds were taken at different intervals by the smart phone camera.

3. Results and Discussion

3.1. Characterization of Prepared CS/GA NPs

The intermolecular interactions can be characterized by Fourier infrared spectroscopy. The infrared spectra of CS, GA and CS/GA are shown in Figure 1.

Compared to CS and GA, CS/GA exhibits significant changes at the amine and carboxyl groups, with the disappearance of the −COO stretching vibration peak at 1732 cm^{-1}, the weakening of the $-NH_3^+$ in-plane bending vibration peak at 1628 cm^{-1}, and the enhancement of the amide C=O stretching vibration at 1623 cm^{-1}. This indicates that the complex is formed mainly by the electrostatic interaction of $-NH_3^+$ of CS and −COO of GA, and no new peaks are observed, indicating no chemical interaction.

Different mixing ratios of chitosan and gum Arabic have different effects on the particle size of nanoparticles. In Figure 2, when the ratio are 4:1, 2:1, 1:2 and 1:4, there are double peaks, and the peak shape is wide and the particle size distribution is wide. In contrast, the peak at the ratio of 1:1 is single and sharp, the particle size distribution is narrow, appearing at 81.96 nm. The possible reason is that the molecular weight of CS used in this experiment is about 200,000, and the molecular weight of GA is about 200,000 as well. Therefore, under the mass ratio of 1:1, chitosan and Arabic gum can form alternating aggregation with a single peak, but they cannot form aggregates with uniform particle size under other proportions.

The contact angle measurement phase results of CS/GA NPs show that with the increase of the proportion of gum Arabic in the nanoparticle composition,

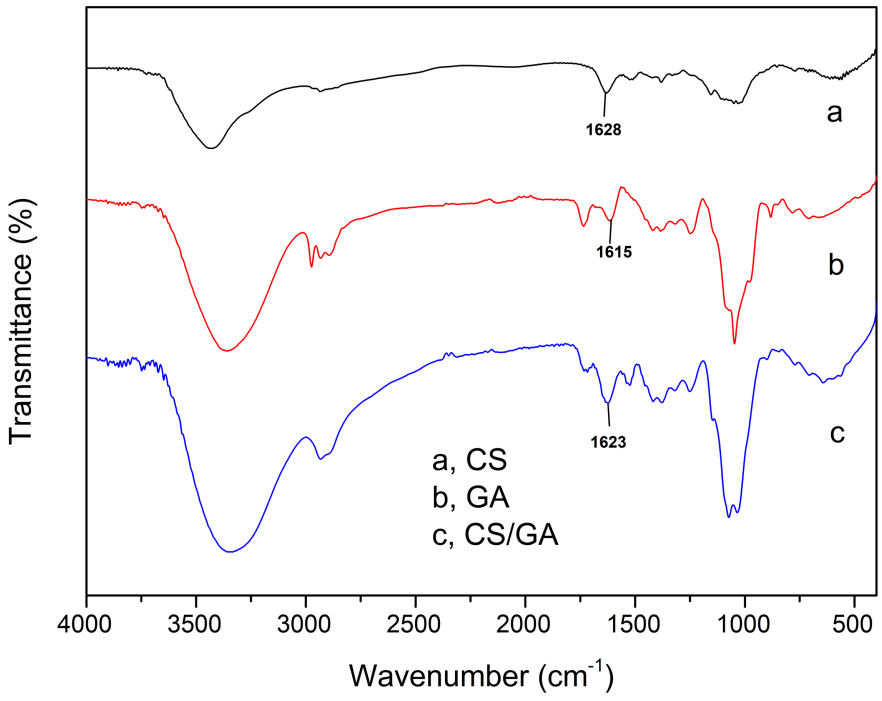

Figure 1. FTIR spectra of (a) CS, (b) GA and (c) CS/GA NPs.

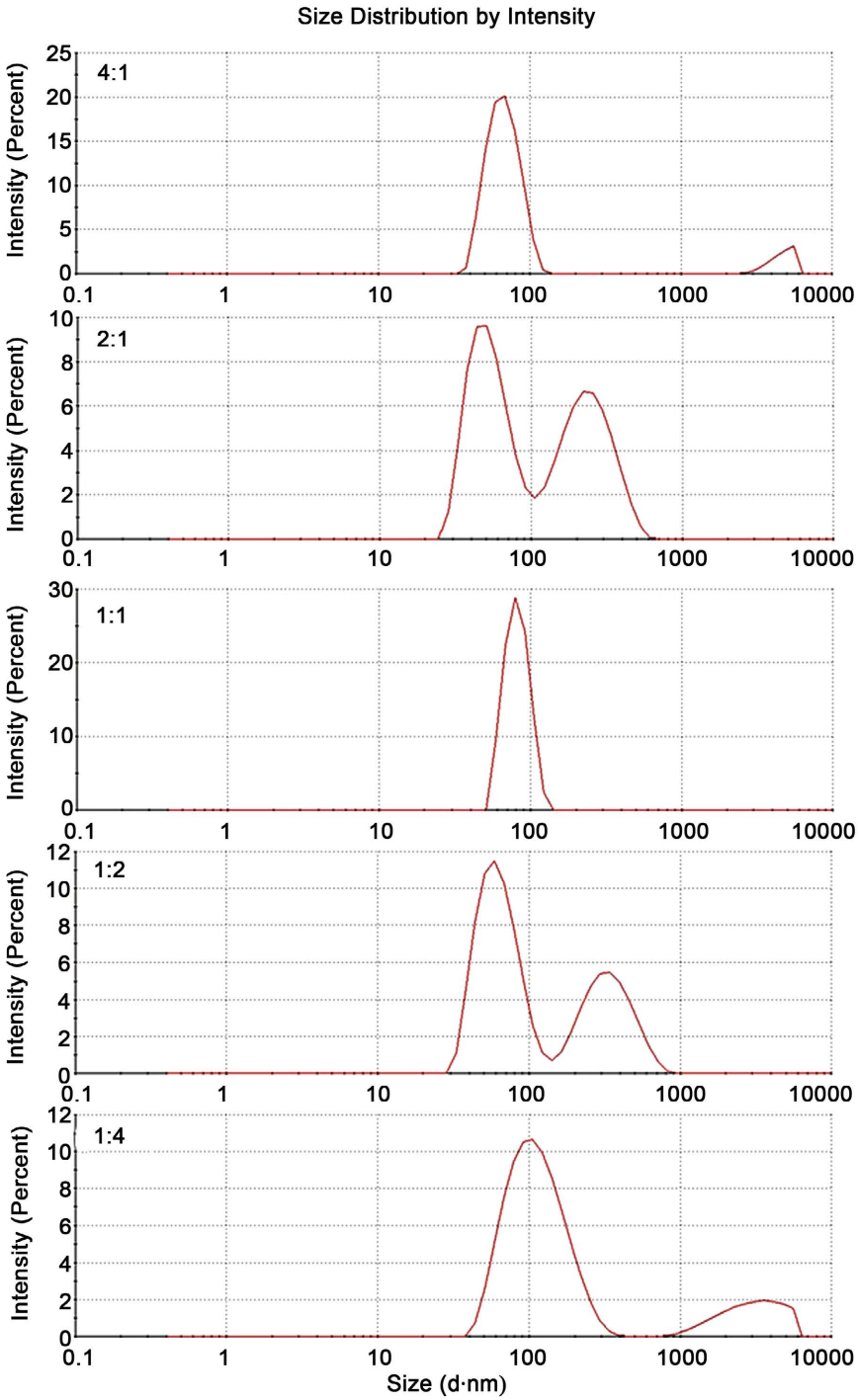

Figure 2. Particle size distribution of CS/GA NPs with different proportions.

the degree of contact angle shows an upward trend (**Figure 3**). When the ratio of CS and GA is 1:4, the contact angle increases the value of the angle is 93.92˚ ± 0.04˚. It has been reported that chitosan nanoparticles have a contact angle of 42.47˚ ± 1.19˚ [15]. The reason for this phenomenon may be that the presence of hydrophobic polypeptide chains in the arabinogalactans protein component in the gum Arabic structure improves the hydrophobicity of CS/GA nanoparticles.

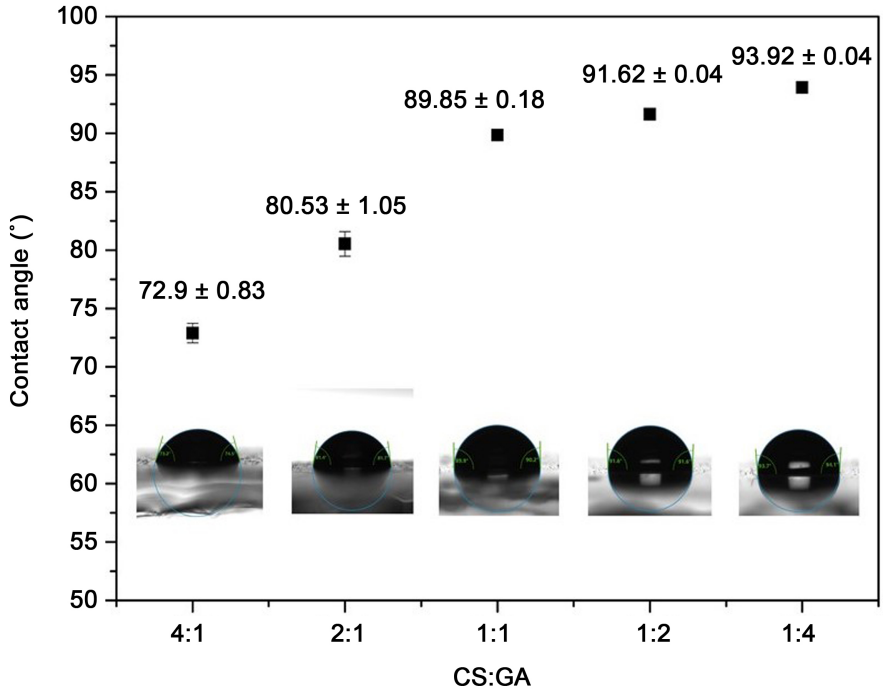

Figure 3. Contact angle of CS/GA NPs with different proportions.

In addition, when the CS/GA mass ratio is 1:1, the contact angle is closest to 90˚, indicating that it has a better tendency to stabilize oil-water emulsions.

The TEM image shows that the nanoparticles are irregular oval or spherical, the surface is relatively rough, and the average particle size is about 80 - 100 nm (**Figure 4**).

3.2. Characterization of Prepared Pickering Emulsions

Different ratios of chitosan/Arabic gum lead to differences in the hydrophilicity and hydrophobicity of nanoparticles, which reflects in the change of contact angle. The closer the contact angle is to 90˚, the easier the nanoparticles are to be stabilized at the oil-water interface, thus making the prepared emulsion more stable. **Figure 5(A)** shows the long-term stability of Pickering emulsions with CS/GA ratios of 1:4, 1:2, 1:1, 4:1, and 2:1, respectively. After standing for 30 days, the emulsions with the ratio of 1:1 chitosan/Arabic gum show no delamination phenomenon, which is the most stable and ideal group.

In normal emulsion systems, droplet size decreases and stability increases with increasing surfactant concentration [20]. Similarly for Pickering emulsions, emulsion size decreases and stability increases with increasing particle concentration. As shown in **Figure 5(B)**, when the particle concentration is 0.5%, the emulsion is very unstable and shows significant delamination on the 7th day of placement, after which the creaming index gradually increased in **Table 1**, indicating that the amount of particles in the dispersed phase is not sufficient to stabilize the emulsion. When the particle concentrations are 1.5% and 3%, no delamination is observed within 30 days, indicating that the number of particles in

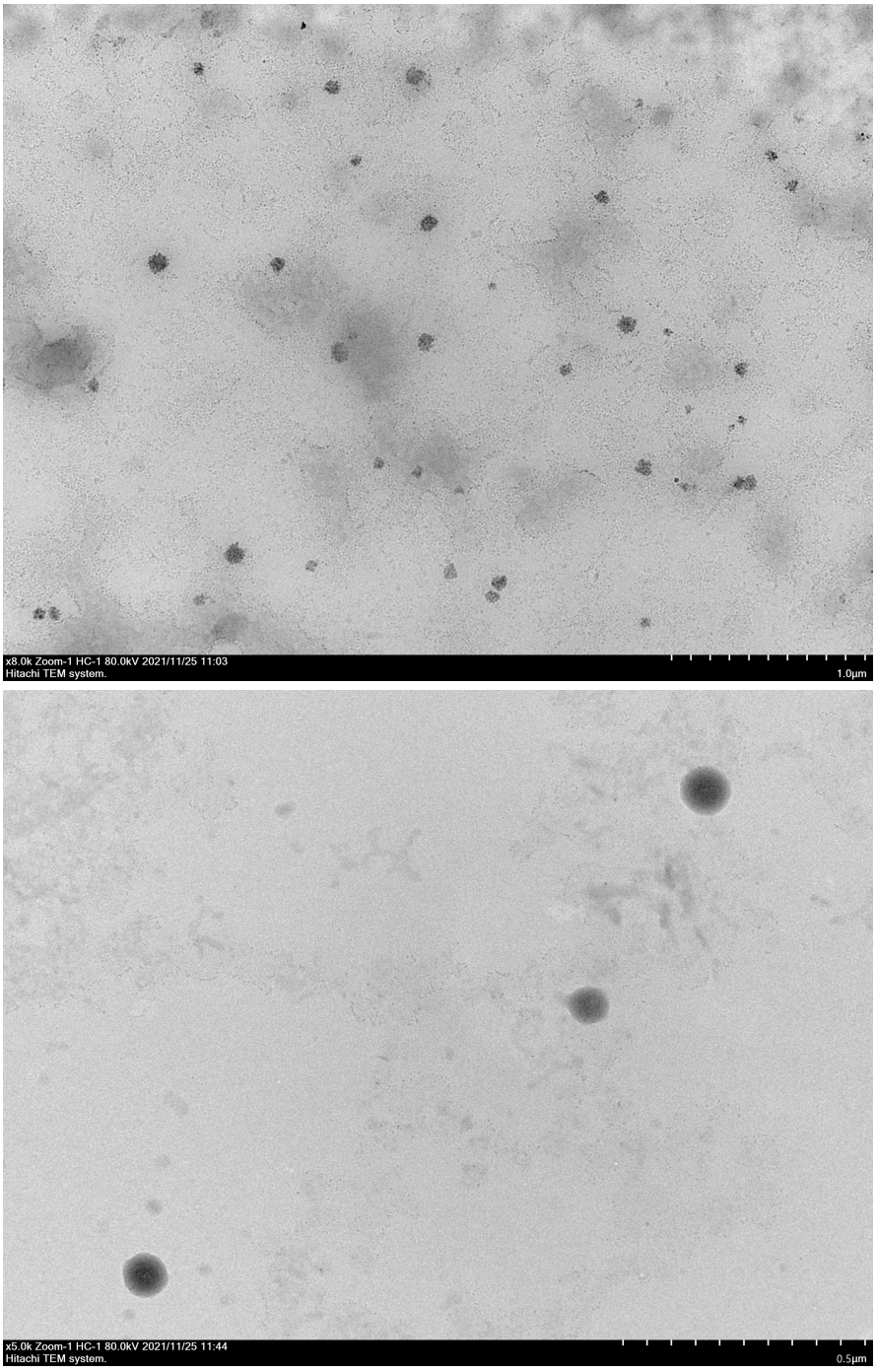

Figure 4. TEM pictures of CS/GA nanoparticles.

both concentrations are sufficient to stabilize the emulsion. The volume ratio of the dispersed phase to the dispersed medium is called the compatibility product ratio, and the emulsion delamination is related to this value. Generally, the delamination speed is inversely proportional to the phase volume ratio. When the phase volume is too small, the emulsion will stratify quickly. With the increasing of the oil-phase ratio, the movement space of the emulsion droplets is small, and the emulsion develops towards stability. As shown in **Figure 5(C)** and **Table 1**,

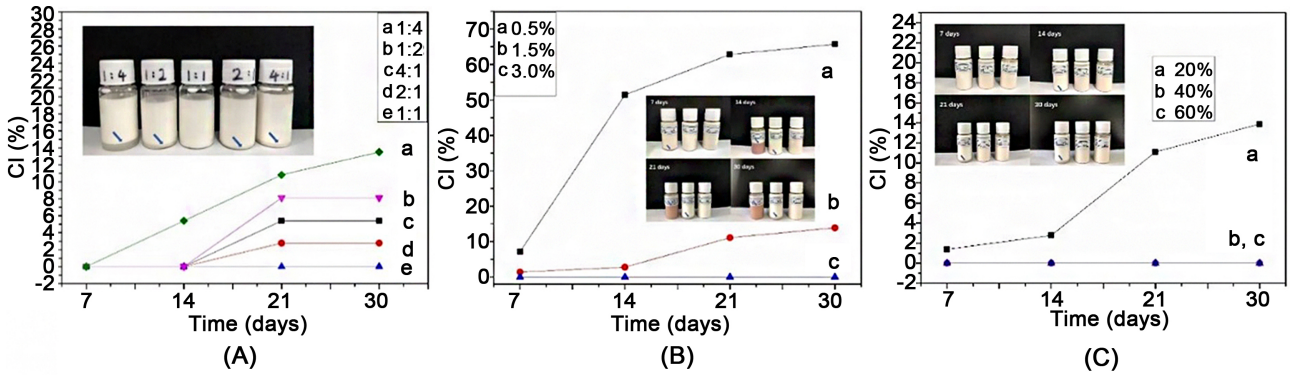

Figure 5. Diagram of stability results, (A) different CS/GA ratios, (B) different concentration, (C) different oil-water ratio.

the emulsions are most stable when the oil phase ratio is 40% and 60%, and there is no emulsification. However, the particle size of the emulsion with 60% oil phase ratio is larger than that of the emulsion with 40% oil phase ratio, so when the CS/GA ratio is 1:1 and the concentration is 1.5%, the emulsion prepared with 40% oil phase ratio is chosen to be the most stable, which can be stored for at least 10 months with no delamination.

3.3. Entrapment Efficiency and Loading Content

After demulsification and centrifugation of Pickering emulsion, the absorbance of VE is measured and substituted into its standard curve Y = 2.6183X + 0.1848 to obtain the drug content, and then the encapsulation efficiency and drug loading capacity. The results are demonstrated in **Table 2**; the encapsulation efficiency of classical emulsion is 91.34% ± 0.75% and the drug loading is 0.177% ± 0.007%, while the encapsulation efficiency of Pickering emulsion is 94.54% ± 0.62% and the drug loading is 0.187% ± 0.009%. The encapsulation efficiency and drug loading of Pickering emulsion stabilized by CS/GA nanoparticles are significantly better than that of ordinary emulsion stabilized by Tween 80 and glycerol, indicating that the 1.5% (w/v) concentration of CS/GA nanoparticles is sufficient to establish a barrier at the oil-water interface and can successfully encapsulate VE in the oil phase.

3.4. *In Vitro* Vitamin E Release Study

It can be seen from **Figure 6** that the cumulative penetration (Q_{24}) of VE per unit area in 24 hours in VE-PE and VE-CE is similar. The release rate of VE-PE group is more gentle in 24 hours, which may be due to the slow release effect of the drug caused by the solid particle shells composed of macromolecules such as chitosan and gum Arabic. The release of VE-CE group increased significantly from the 2nd hour to the 6th hour. It might be that Tween 80, a surfactant in CE, changed the integrity of the lipid layer of the stratum corneum, weakened the barrier function of the stratum corneum, and temporarily increased the drug penetration rate.

According to the 24-h cumulative permeability per unit area of VE in PE and

Table 2. Encapsulation and loading content of emulsion ($\bar{X}$ ± SD).

Emulsion	EE %	LC %
PE	94.54 ± 0.62	0.1872 ± 0.86
CE	91.34 ± 0.75	0.1770 ± 0.75

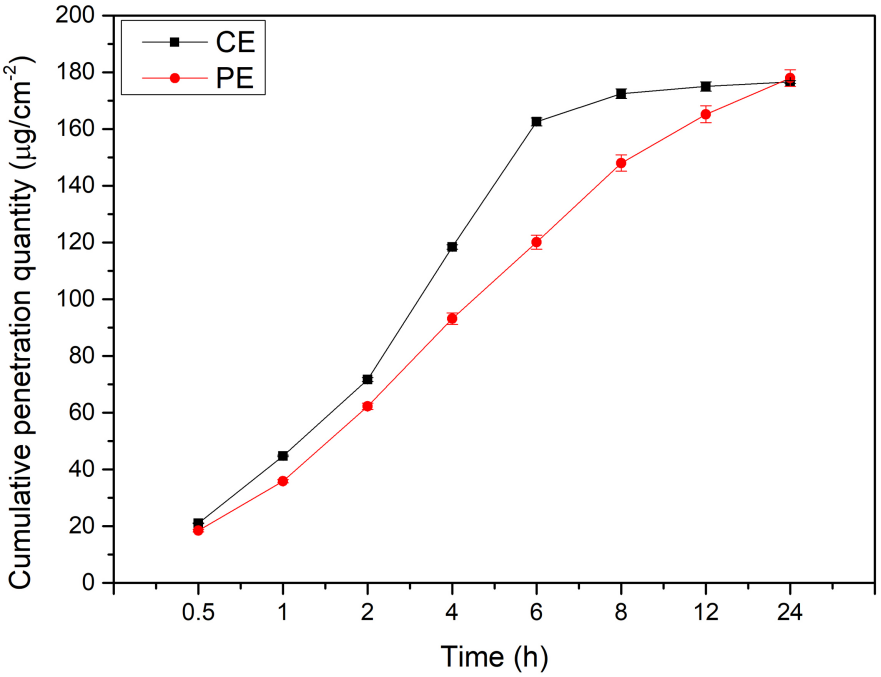

Figure 6. A curve diagram of the cumulative permeability-time of basic remedy *in vitro* (n = 3).

CE measured, with the sampling time t(h) as the abscissa, the cumulative permeability per unit area Q_{24} (μg/cm^2) as the ordinate, we plotted the cumulative release of VE in PE and CE in vitro. From **Figure 7** and **Table 3**, it can be concluded that the in vitro cumulative release kinetics of VE in PE and CE conform to the first-order equation; that is, the whole release process is more consistent with the slow-release mode.

3.5. *In Vitro* Bacteriostatic Test

Figure 8 is a histogram of the diameter of the inhibition zone of tea tree oil, classical emulsion, edible olive oil, CS/GA nanoparticles and Pickering emulsion against four strains. **Figure 9** is a visual diagram of the diameter of the inhibition zone of the five substances on different strains. Compared to the edible olive oil group, CS/GA NPs group and tea tree oil group both showed a certain bacteriostatic effect on these four bacteria. But after tea tree oil is made into the classical emulsion and Pickering emulsion stabilized by CS/GA NPs, respectively, there is no significant change in the size of the inhibition zone of the four bacteria in the ordinary emulsion compared with tea tree oil alone. However, the inhibition zone of Pickering emulsion is all significantly enlarged, indicating that the

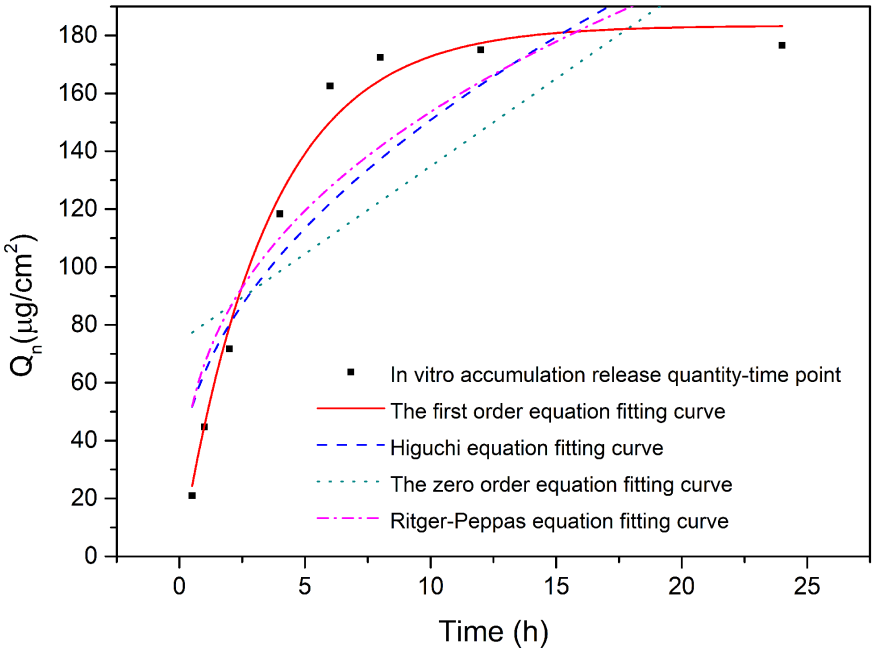

(A)

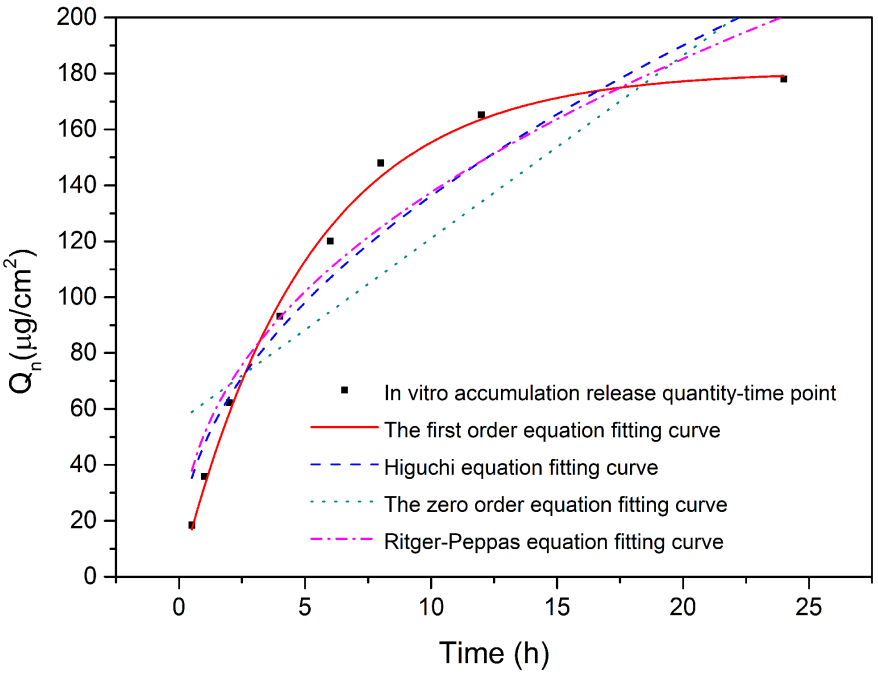

(B)

Figure 7. A fitting curve diagram of the cumulative permeability amount - time curve of VE in emulsion (A) PE. (B) CE.

CS/GA NPs and tea tree oil can simultaneously exert synergistic antibacterial effects.

3.6. *In Vivo* Anti-Inflammatory Test

The *In Vivo* anti-inflammatory effect of VE Pickering emulsion is investigated

Table 3. A summary table of the fitting results of the external release kinetics of VE in PE and CE.

Material	Kinetic Model	Fit Equation	R2
PE	Zero-order model	Q_n = 74.2859 + 6.0541t	0.4746
	First-order model	Q_n = 183.4176 (1-e-0.2845t)	0.9846
	Higuchi model	Q_n = 23.1602 + 40.3532t1/2	0.7318
	Ritger-Peppas model	Q_n = 66.6792t0.3624	0.7890
CE	Zero-order model	Q_n = 55.6014 + 6.5418t	0.6806
	First-order model	Q_n = 180.7749 (1-e-0.1960t)	0.9951
	Higuchi model	Q_n = 6.2254 + 41.1017t1/2	0.8881
	Ritger-Peppas model	Q_n = 51.0505t0.4303	0.9050

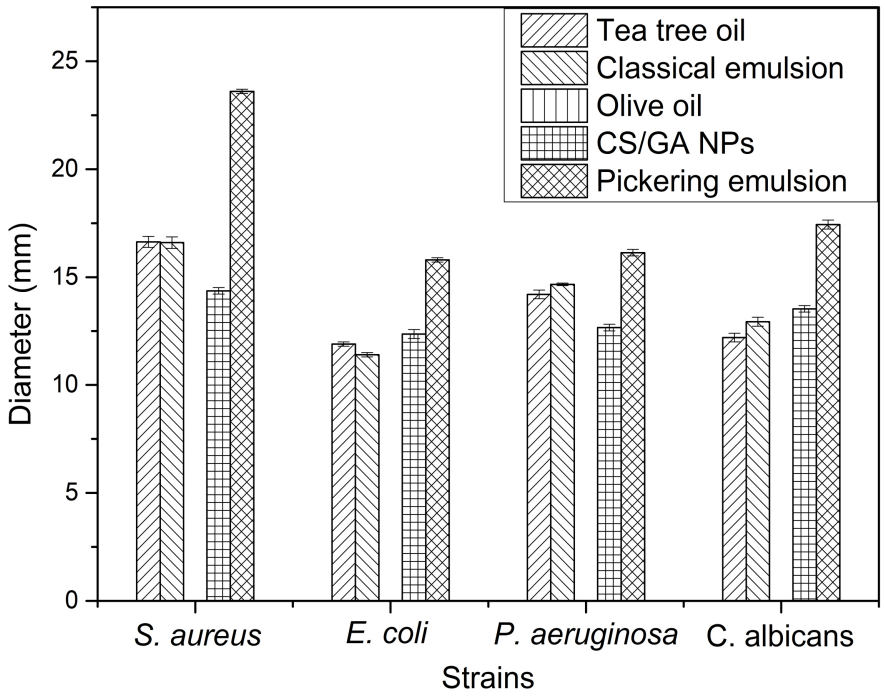

Figure 8. Diameter of tea tree oil, common emulsion, chitosan, CS/GA nanoparticles and Pickering emulsion against four bacteria.

using an acute inflammation model in which acetic acid induces peritoneal vascular permeability. In this experiment, the content of Evans blue is used as an indicator of peritoneal vascular permeability. The lower the vascular permeability, the less Evans blue content, which indicates the stronger the inhibition. As shown in **Table 4**, both the medium-dose and high-dose groups of VE Pickering emulsion significantly reduce the peritoneal permeability of mice with Evans blue content of 3.06 ± 0.0035 μg/mL and 1.58 ± 0.0016 μg/mL, and the inhibition rate is 64.13% and 81.48%, respectively. And at the same dose, there is little difference in the inhibition rate between the medium dose group (64.13%) and the control group (71.16%). It indicates that Pickering emulsion with a specific

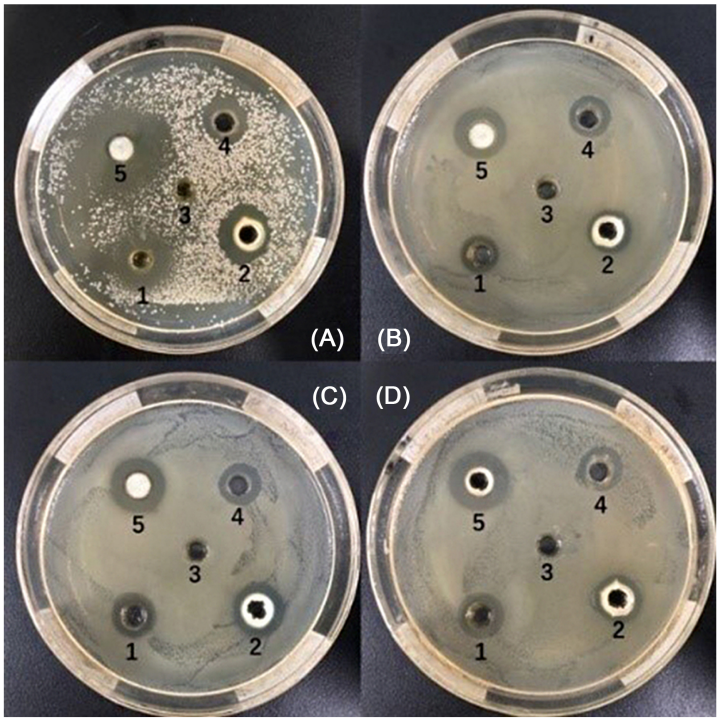

Figure 9. Diameter of (A) *Staphylococcus aureus* (B) *Escherichia coli* (C) *Pseudomonas aeruginosa* (D) *Candida albicans*. (1) Tea tree oil (2) CE (3) Olive oil (4) CS/GA NPs (5) PE.

Table 4. Date of acetic acid induced Evans blue peritoneal permeability.

Group	Dose (g/kg)	Evans blue concentration ± SD (μg/mL)	Inhibition rate (%)
Blank group	0	8.53 ± 0.0021	-
Low concentration	1.2	7.22 ± 0.0031	15.36
Middle concentration	2.4	3.06 ± 0.0035	64.13
High concentration	4.8	1.58 ± 0.0016	81.48
Control group	2.4	2.46 ± 0.0021	71.16

amount of VE has a significant inhibitory effect on acetic acid-induced increase in vascular permeability in the peritoneal cavity of mice, and it has a good acute anti-inflammatory effect.

3.7. Wound Healing Test

Figure 10 reflects the healing process of the wounds. Among them, the wound area treated with Pickering emulsion was the smallest on day 5, and healed completely on day 10. Table 5 shows the wound healing rate corresponding to different drugs. The healing rate of the Pickering emulsion group was the highest on the 5th and 10th day, and the improvement of the healing rate was especially obvious compared with the blank group. Even compared with the CE Group, the effect of PE on wound healing was significantly higher ($p < 0.001$).

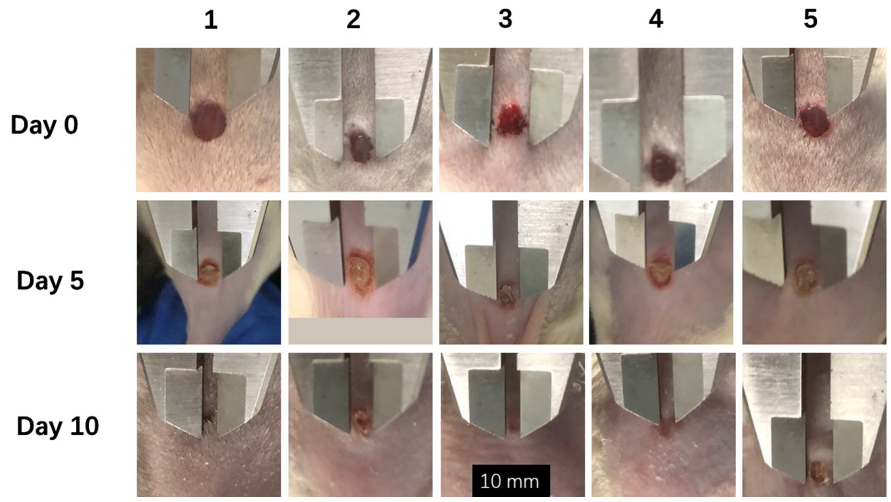

Figure 10. The picture of wound healing in different time periods (1) Pickering emulsion (2) Classical emulsion (3) CS/GA nanoparticles (4) Tea tree oil (5) Blank group.

Table 5. Wound healing rate of different media.

Group	Wound healing (%)	
	Day 5	Day 10
PE	49.68 ± 1.86****	90.72 ± 1.15****
CE	24.4 ± 1.26	72.8 ± 0.63
CS/GA NPs	29.52 ± 1.21	87.44 ± 1.40
Tea tree oil	17.68 ± 1.66	82.08 ± 0.72
Blank	15.12 ± 1.00	63.04 ± 1.15

****Indicates an extremely significant difference ($p < 0.001$).

4. Conclusion

In summary, Pickering emulsion with good antibacterial, anti-inflammatory and healing effects was successfully fabricated. This Pickering emulsion was stabilized by CS/GA nanoparticles and composed of water and tea tree oil. In the stability test, the emulsions showed good stability, which made them easy to store. In addition, Pickering emulsion had effective inhibition towards *Staphylococcus aureus*, *Escherichia coli*, *Pseudomonas aeruginosa* and *Candida albicans*. Besides, it also showed a good anti-inflammatory effect *in Vivo*. In the study of the wound healing model, Pickering emulsion had the most obvious healing effect, especially compared with classical emulsion. All the results indicated that the CS/GA based Pickering emulsions are a promising candidate for wound healing. Notably, further systematic research can be carried out on this Pickering emulsion, such as a system consisting of adjacent concentrations of each component or loading specific drugs for different situations.

Conflicts of Interest

The authors report no conflicts of interest in this work.

References

[1] Schreml, S., Szeimies, R.-M., Prantl, L., Landthaler, M. and Babilas, P. (2010) Wound Healing in the 21st Century. *Journal of the American Academy of Dermatology*, **63**, 866-881. https://doi.org/10.1016/j.jaad.2009.10.048

[2] Gainza, G., Bonafonte, D.C., Moreno, B., Aguirre, J.J., Gutierrez, F.B., Villullas, S., Pedraz, J.L., Igartua, M. and Hernandez, R.M. (2015) The Topical Administration of rhEGF-Loaded Nanostructured Lipid Carriers (rhEGF-NLC) Improves Healing in a Porcine Full-Thickness Excisional Wound Model. *Journal of Controlled Release*, **197**, 41-47. https://doi.org/10.1016/j.jconrel.2014.10.033

[3] Tenci, M., Rossi, S., Bonferoni, M.C., Sandri, G., Boselli, C., Lorenzo, A.D., Daglia, M., Cornaglia, A., Gioglio, L., Perotti, C., Caramella, C. and Ferrari, F. (2016) Particulate Systems Based on Pectin/Chitosan Association for the Delivery of Manuka Honey Components and Platelet Lysate in Chronic Skin Ulcers. *International Journal of Pharmaceutics*, **509**, 59-70. https://doi.org/10.1016/j.ijpharm.2016.05.035

[4] Zheng, B.-D., Ye, J., Yang, Y.-C., Huang, Y.-Y. and Xiao, M.-T. (2022) Self-Healing Polysaccharide-Based Injectable Hydrogels with Antibacterial Activity for Wound Healing. *Carbohydrate Polymers*, **275**, Article ID: 118770. https://doi.org/10.1016/j.carbpol.2021.118770

[5] Venkataprasanna, K.S., Prakash, J., Mathapati, S.S., Bharath, G., Banat, F. and Venkatasubbu, G.D. (2021) Development of Chitosan/Poly (Vinyl Alcohol)/Graphene Oxide Loaded with Vanadium Doped Titanium Dioxide Patch for Visible Light Driven Antibacterial Activity and Accelerated Wound Healing Application. *International Journal of Biological Macromolecules*, **193**, 1430-1448. https://doi.org/10.1016/j.ijbiomac.2021.10.207

[6] Wu, G., Ma, F., Xue, Y., Peng, Y., Hu, L., Kang, X., Sun, Q., Ouyang, D.F., Tang, B. and Lin, L. (2022) Chondroitin Sulfate Zinc with Antibacterial Properties and Anti-Inflammatory Effects for Skin Wound Healing. *Carbohydrate Polymers*, **278**, 118996. https://doi.org/10.1016/j.carbpol.2021.118996

[7] Saputro, I.D., Rizaliyana, S. and Noverta, D.A. (2022) The Effect of Allogenic Freeze-Dried Platelet-Rich Plasma in Increasing the Number of Fibroblasts and Neovascularization in Wound Healing. *Annals of Medicine and Surgery*, **73**, Article ID: 103217. https://doi.org/10.1016/j.amsu.2021.103217

[8] Ortiz, D.G., Pochat-Bohatier, C., Cambedouzou, J., Bechelany, M. and Miele, P. (2022) Current Trends in Pickering Emulsions: Particle Morphology and Applications. *Engineering*, **6**, 468-482. https://doi.org/10.1016/j.eng.2019.08.017

[9] Bao, X., Wu, J. and Ma, G. (2020) Sprayed Pickering Emulsion with High Antibacterial Activity for Wound Healing. *Progress in Natural Science*: *Materials International*, **30**, 669-676. https://doi.org/10.1016/j.pnsc.2020.08.001

[10] Chevalier, Y. and Bolzinger M.-A. (2013) Emulsions Stabilized with Solid Nanoparticles: Pickering Emulsions. *Colloids and Surfaces A*: *Physicochemical and Engineering Aspects*, **439**, 23-34. https://doi.org/10.1016/j.colsurfa.2013.02.054

[11] Qi, J., Gong, M., Zhang, R., Song, Y., Liu, Q., Zhou, H., Wang, J. and Mei, Y. (2021) Evaluation of the Antibacterial Effect of Tea Tree Oil on *Enterococcus faecalis* and Biofilm in Vitro. *Journal of Ethnopharmacology*, **281**, Article ID: 114566. https://doi.org/10.1016/j.jep.2021.114566

[12] Zhang, F., Ramachandran, G., Mothana, R.A., Noman, O.M., Alobaid, W.A., Rajivgandhi, G. and Manoharan, N. (2020) Anti-Bacterial Activity of Chitosan Loaded Plant Essential Oil against Multi Drug Resistant *K. pneumonia*. *Saudi Journal of Biological Sciences*, **27**, 3449-3455. https://doi.org/10.1016/j.sjbs.2020.09.025

[13] Semeniuc, C.A., Pop, C.R. and Rotar, A.M. (2017) Antibacterial Activity and Interactions of Plant Essential Oil Combinations against Gram-Positive and Gram-Negative Bacteria. *Journal of Food and Drug Analysis*, **25**, 403-408. https://doi.org/10.1016/j.jfda.2016.06.002

[14] Fan, L., Yang, H., Yang, J., Peng, M. and Hu, J. (2016) Preparation and Characterization of Chitosan/Gelatin/PVA Hydrogel for Wound Dressings. *Carbohydrate Polymers*, **146**, 427-434. https://doi.org/10.1016/j.carbpol.2016.03.002

[15] Asfour, M.H., Elmotasem, H., Mostafa, D.M. and Salama, A.A.A. (2017) Chitosan Based Pickering Emulsion as a Promising Approach for Topical Application of Rutin in a Solubilized Form Intended for Wound Healing: *In Vitro* and *In Vivo* Study. *International Journal of Pharmaceutics*, **534**, 325-338. https://doi.org/10.1016/j.ijpharm.2017.10.044

[16] Rhazi, L., Lakahal, L., Andrieux, O., Niamba, N., Depeint, F. and Guillemet, D. (2020) Relationship between the Molecular Characteristics of *Acacia* Gum and Its Functional Properties. *Food Chemistry*, **328**, Article ID: 126860. https://doi.org/10.1016/j.foodchem.2020.126860

[17] Harun, M.S., Wong, T.W. and Fong, C.W. (2021) Advancing Skin Delivery of α-Tocopherol and γ-Tocotrienol for Dermatitis Treatment via Nanotechnology and Microwave Technology. *International Journal of Pharmaceutics*, **593**, Article ID: 120099. https://doi.org/10.1016/j.ijpharm.2020.120099

[18] Praça, F.G., Viegas, J.S.R., Peh, H.Y., Garbin, T.N., Medina, W.S.G. and Bentley, M.V.L.B. (2020) Microemulsion Co-Delivering Vitamin A and VE as a New Platform for Topical Treatment of Acute Skin Inflammation. *Materials Science and Engineering*: *C*, **110**, Article ID: 110639. https://doi.org/10.1016/j.msec.2020.110639

[19] Catanzano, O., Straccia, M.C., Miro, A., Ungaro, F., Romano, I., Mazzarella, G., Santagata, G., Quaglia, F., Laurienzo, P. and Malinconico, M. (2015) *Spray-by-Spray in Situ* Cross-Linking Alginate Hydrogels Delivering a Tea Tree Oil Microemulsion. *European Journal of Pharmaceutical Sciences*, **66**, 20-28. https://doi.org/10.1016/j.ejps.2014.09.018

[20] Nesterenko, A., Drelich, A., Lu, H., Clausse, D. and Pezron, I. (2014) Influence of a Mixed Particle/Surfactant Emulsifier System on Water-in-Oil Emulsion Stability. *Colloids and Surfaces A*: *Physicochemical and Engineering Aspects*, **457**, 49-57. https://doi.org/10.1016/j.colsurfa.2014.05.044